AFRL-RV-PS-
TR-2015-0115

CHARACTERIZATION OF RAIN ATTENUATION AND DEPOLARIZATION AT W/V BANDS

Christos Christodoulou

Department of Electrical and Computer Engineering
University of New Mexico
Albuquerque, NM 87131

30 July 2015

Final Report

AIR FORCE RESEARCH LABORATORY
Space Vehicles Directorate
3550 Aberdeen Ave SE
AIR FORCE MATERIEL COMMAND
KIRTLAND AIR FORCE BASE, NM 87117-5776

DTIC COPY
NOTICE AND SIGNATURE PAGE

This report is the result of contracted fundamental research deemed exempt from public affairs security and policy review in accordance with SAF/AQR memorandum dated 10 Dec 08 and AFRL/CA policy clarification memorandum dated 16 Jan 09. This report is available to the general public, including foreign nationals. Copies may be obtained from the Defense Technical Information Center (DTIC) (http://www.dtic.mil).

AFRL-RV-PS-TR-2015-0115 HAS BEEN REVIEWED AND IS APPROVED FOR PUBLICATION IN ACCORDANCE WITH ASSIGNED DISTRIBUTION STATEMENT.

//SIGNED//
STEVEN A. LANE
Program Manager

//SIGNED//
PAUL HAUSGEN, Ph.D.
Technical Advisor, Space Based Advanced Sensing and Protection

//SIGNED//
JOHN BEAUCHEMIN
Chief Engineer, Spacecraft Technology Division
Space Vehicles Directorate

This report is published in the interest of scientific and technical information exchange, and its publication does not constitute the Government's approval or disapproval of its ideas or findings.

REPORT DOCUMENTATION PAGE

Form Approved
OMB No. 0704-0188

1. REPORT DATE *(DD-MM-YYYY)*	**2. REPORT TYPE**	**3. DATES COVERED** *(From - To)*
30-07-2015	Final Report	01 May 2014 to 30 Jul 2015

4. TITLE AND SUBTITLE

Characterization of Rain Attenuation and Depolarization at W/V Bands

5a. CONTRACT NUMBER
FA9453-14-1-0238

5b. GRANT NUMBER

5c. PROGRAM ELEMENT NUMBER
61102F

6. AUTHOR(S)

Christos Christodoulou

5d. PROJECT NUMBER
3001

5e. TASK NUMBER
PPM00019618

5f. WORK UNIT NUMBER
EF122382

7. PERFORMING ORGANIZATION NAME(S) AND ADDRESS(ES)
Department of Electrical and Computer Engineering
University of New Mexico
Albuquerque, NM 87131

8. PERFORMING ORGANIZATION REPORT NUMBER

9. SPONSORING / MONITORING AGENCY NAME(S) AND ADDRESS(ES)
Air Force Research Laboratory
Space Vehicles Directorate
3550 Aberdeen Ave SE
Kirtland AFB, NM 87117-5776

10. SPONSOR/MONITOR'S ACRONYM(S)
AFRL/RVSV

11. SPONSOR/MONITOR'S REPORT NUMBER(S)
AFRL-RV-PS-TR-2015-0115

12. DISTRIBUTION / AVAILABILITY STATEMENT

Approved for public release; distribution is unlimited.

13. SUPPLEMENTARY NOTES

14. ABSTRACT

The objective of this research project was to develop a W/V-band Terrestrial Link Experiment (WTLE) for the characterization of rain attenuation at the W/V frequency bands. This test framework can be used to verify and validate models, which can then be used to predict path attenuation, phase distortion, and depolarization at the W/V bands. The first part of this report discusses current models available in the literature. The second part of the report details the work related to setting up the hardware and building the actual test link between two locations. The report ends with conclusions stating the nature of this on-going work and the future research to be completed.

15. SUBJECT TERMS
Space communication, satellite communication, W/V-band, radio frequency propagation

16. SECURITY CLASSIFICATION OF:			**17. LIMITATION OF ABSTRACT**	**18. NUMBER OF PAGES**	**19a. NAME OF RESPONSIBLE PERSON**
a. REPORT	**b. ABSTRACT**	**c. THIS PAGE**			Steven A. Lane
Unclassified	Unclassified	Unclassified	Unlimited	46	**19b. TELEPHONE NUMBER** *(include area code)*

(This page intentionally left blank)

TABLE OF CONTENTS

LIST OF FIGURES

LIST OF TABLES

ACKNOWLEDGMENTS

This material is based on research sponsored by Air Force Research Laboratory under agreement number FA9453-14-1-0238. The U.S. Government is authorized to reproduce and distribute reprints for Governmental purposes notwithstanding any copyright notation thereon.

DISCLAIMER

The views and conclusions contained herein are those of the authors and should not be interpreted as necessarily representing the official policies or endorsements, either expressed or implied, of Air Force Research Laboratory or the U.S. Government.

1 SUMMARY

This grant focused on investigating effects of the atmosphere on electromagnetic signal propagation at W-band (81 – 86 GHz) and V-band (71 – 76 GHz). We compared modeling approaches that included dry air (gases), water vapor, fog, clouds, and rain. We developed laboratory test facilities to characterize antenna performance at these frequencies. We developed a slant-path experiment to measure the effects of weather and assess model accuracy. The goal is that through this experiment, a reliable attenuation model can be constructed (or verified) to indicate the amount of attenuation a specific terrestrial link would have at these frequencies. This could then be applied to satellite communication link modeling.

2 INTRODUCTION

The W-band (81 – 86 GHz) and V-band (71 – 76 GHz) frequency bands have potential to provide very high bandwidth (i.e., gigabit per second (Gbps) data rates), point-to-point communications between a satellite and a ground station [1-4]. However, one of the most critical problems in achieving this type of communication link is the uncertainty of signal attenuation, depolarization, and phase distortion that results from atmospheric absorption, scintillation, and meteorological effects (e.g., rain-fade, atmospheric and molecular absorption, and scattering from hydrometers). Rain parameters such as drop-size, drop-shape and canting angle can impact the propagation of waves at such extremely high frequencies. As rainfall affects the propagation of the wave, rainfall itself is also affected by several other factors, such as wind velocity and temperature [5-7]. During a turbulent condition, a vertical wind velocity component is present, and the raindrop density in the microwave beam does not change, but the rain-rate measured at the ground changes considerably [8-12], which causes uncertainty in the correlation of attenuation and rain-rate measurements. Furthermore, the overall dielectric constant of rainfall water is altered with temperature, thus changing the values of the attenuation coefficient.

There are several approaches that scientists have used in the past to estimate rain attenuation based on the use of a large number of attenuation variations at different frequencies, locations, and path geometries. Additionally, there are several predictive models that are based on theoretical evaluation and extrapolations to higher frequencies using lower frequency observations. Our goal in this work was to devise an experiment to collect attenuation and

depolarization data directly at the W/V-bands so high-fidelity propagation models can be developed and statistically validated. Our proposed terrestrial link experiment (simply referred to as W/V-band Terrestrial Link Experiment, or WTLE) would enable the measurement of attenuation, rain-rate, and rain-drop size distribution using the receiver and weather sensors. The two main parameters of interests that are expected to be measured using this terrestrial link are: (1) rain attenuation and (2) depolarization.

Attenuation is usually modeled by the power law relationship given by:

$$A = \alpha R\beta, \tag{1}$$

where A is the attenuation due to rain, in dB/km, R is the rain rate, in mm/hr, and α and β are constants that depend on parameters such as frequency, rain, temperature, and rain drop size distribution [13]. Depolarization of a propagating electromagnetic wave is usually due to the presence of ice crystals at high altitudes (typically greater than 2-km) and rain at lower altitudes (less than 2-km). In general, depolarization of a propagating signal can be modeled in terms of the scattered-field matrix as:

$$[E_s] = e^{-(a_n - j\phi_n)L}[E_i], \tag{2}$$

where L is the path length through the scattering region, $[E_i]$ is the incident field vector, $[E_s]$ is the scattered field vector, and a_n and ϕ_n are the attenuation and phase-lag vector components, respectively. These components are dependent on the rain-drop geometry and distribution. Both, the attenuation and depolarization constants vary statistically depending on local weather. Therefore, it is important that the WTLE setup collects adequate data to enable studies of rain attenuation over many rain events, with a reliable knowledge of rain-rate and rain-drop size distribution.

We investigated the International Telecommunications Union (Radio) (ITU-R) models for rain [14], atmospheric gases [15], and clouds or fog [16] attenuation. These models were developed by researchers over many years and have been verified using data collected world-wide. For comparison, we investigated a model developed by Luis da Silva Mello that includes path attenuation due to rain attenuation [17]. Comparisons at two frequencies (72 GHz and 82 GHz) were made and included in this report. Simulation results are presented for the proposed WTLE experiment. To incorporate realistic data for the models of the specific link, weather data from local weather stations were accessed via the Mesowest website [18]. Water vapor densities

were also found through an ITU-R database [19] and a related ITU-R water vapor density paper [20].

Details of the WTLE test are described in this report. The WTLE tests are planned to be conducted in Albuquerque, New Mexico, later in 2015. The transmit assembly and receive assembly, along with the related equipment, are described in detail. A discussion of the antenna test fixtures and other hardware fixtures that we developed to calibrate the antenna is presented.

3 METHODS, ASSUMPTIONS, AND PROCEDURES

3.1 ITU-R Model

3.1.1 Atmospheric Gases

One of the factors affecting the propagating signal is the attenuation due to atmospheric gases, such as nitrogen, oxygen, and water vapor. The ITU-R reference: "Attenuation by Atmospheric Gases" provided a model for these atmosphere constituents [15]. This reference provided two different methods to estimate the attenuation on terrestrial and slant paths. The method applied herein was a simplified approximation for the frequency range of 1-350 GHz. The total (combined) *specific attenuation* (i.e., dB/km) due to atmospheric gases was estimated using a simplified algorithm based on curve-fitting to the line-by-line calculation of attenuation by dry air and by water vapor.

For dry air (i.e., no water vapor), the attenuation, γ_0 (dB/km), can be estimated by the following equation:

$$\gamma_0 = \left\{3.02 \times 10^{-4} r_t^{3.5} \frac{0.283 r_t^{3.8}}{(f-118.75)^2+2.91 r_p^2 r_t^{1.6}} + \frac{0.502\xi_6[1-0.0163\xi_7(f-66)]}{(f-66)^{1.4346\xi_4+1.15\xi_5}}\right\} f^2 r_p^2 \times 10^{-3} \quad (3)$$

where:

$$\xi_4 = \varphi\left(r_p, r_t, -0.0112, 0.0092, -0.1033, -0.0009\right), \quad (4)$$

$$\xi_5 = \varphi\left(r_p, r_t, 0.2705, -2.7192, -0.3016, -4.1033\right), \quad (5)$$

$$\xi_6 = \varphi\left(r_p, r_t, 0.2445, -5.9191, 0.0422, -8.0719\right), \quad (6)$$

$$\xi_7 = \varphi\left(r_p, r_t, -0.1833, 6.5589, -0.2402, 6.131\right), \quad (7)$$

f: frequency (GHz),

$r_p = p_{tot}/1013$, where p_{tot} represents total air pressure, (8)

$r_t = 288/(273+t)$, (9)

p: pressure (hPa), and

t: temperature (°C).

For water vapor, the attenuation, γ_w (dB/km), can be estimated by the following equation:

$$\gamma_w = \left\{\frac{3.98\eta_1 \exp[2.23(1-r_t)]}{(f-22.235)^2+9.42\eta_1^2} g(f,22) + \frac{11.96\eta_1 \exp[0.7(1-r_t)]}{(f-183.31)^2+11.14\eta_1^2} + \frac{0.081\eta_1 \exp[6.44(1-r_t)]}{(f-321.226)^2+6.29\eta_1^2} + \frac{3.66\eta_1 \exp[1.6(1-r_t)]}{(f-325.153)^2+9.22\eta_1^2} + \frac{25.37\eta_1 \exp[1.09(1-r_t)]}{(f-380)^2} + \frac{17.4\eta_1 \exp[1.46(1-r_t)]}{(f-448)^2} + \frac{844.6\eta_1 \exp[0.17(1-r_t)]}{(f-557)^2} g(f,557) + \frac{290\eta_1 \exp[0.41(1-r_t)]}{(f-752)^2} g(f,752) + \frac{8.3328\times10^4\eta_2 \exp[0.99(1-r_t)]}{(f-1780)^2} g(f,1780)\right\} f^2 r_t^{2.5} \rho \times 10^{-4} \quad , \tag{10}$$

where:

$$\eta_1 = 0.955 r_p r_t^{0.68} + 0.006\rho, \tag{11}$$

$$\eta_2 = 0.735 r_p r_t^{0.5} + 0.0353 r_t^{0.4} \rho, \tag{12}$$

$$g(f, f_i) = 1 + \left(\frac{f-f_i}{f+f_i}\right)^2, \tag{13}$$

$$\rho = \rho_1 \exp\left(h_1/2\right), \tag{14}$$

and:

ρ: water vapor density (g/m^3),

ρ_1: water vapor density at altitude h_1 of the corresponding station, and

h_1: altitude of the receiving station.

These expressions can be combined to estimate the *total* path attenuation due to dry air and water vapor. For WTLE, propagation path is inclined at an angle of about 4°. Therefore, the procedure presented by the ITU-R to calculate the attenuation of an inclined path having an elevation angle between 0° and 5° was used. Thus, the total attenuation can be estimated by:

$$A = \gamma_0 \sqrt{h_0} \left[\frac{\sqrt{R_e+h_1} F(x_1) e^{-h_1/h_0}}{cos\varphi_1} - \frac{\sqrt{R_e+h_2} F(x_2) e^{-h_2/h_0}}{cos\varphi_2}\right] + \gamma_w \sqrt{h_w} \left[\frac{\sqrt{R_e+h_1} F(x_1') e^{-h_1/h_w}}{cos\varphi_1} - \frac{\sqrt{R_e+h_2} F(x_2') e^{-h_2/h_w}}{cos\varphi_2}\right] \quad , \tag{15}$$

where:

$$F(x) = \frac{1}{0.661x+0.339\sqrt{x^2+5.51}}, \quad (16)$$

$$\varphi_2 = \arccos\left(\frac{R_e+h_1}{R_e+h_2} cos\varphi_1\right), \quad (17)$$

$$x_i = tan\varphi_i \sqrt{\frac{R_e+h_i}{h_0}} for\ i = 1, 2, \quad (18)$$

$$x_i' = tan\varphi_i \sqrt{\frac{R_e+h_i}{h_w}}\ for\ i = 1, 2\ , \quad (19)$$

and

A: total attenuation (dB),

R_e: effective earth radius (8,500 km), and

φ_1: elevation angle at altitude h_1.

Frequency, temperature, and air pressure are factors required to calculate the attenuation from the ITU-R model equations. The altitudes at the reference points are also required

3.1.2 Clouds and Fog

Another factor affecting the propagating signal is attenuation due to clouds and fog, *which is distinct from "water vapor" modeled in the previous section*. To model the effect of cloud and fog, the ITU-R reference: "Attenuation Due to Clouds and Fog" was used [16]. According to the ITU-R paper, if the clouds and fog consist of small droplets less than 0.01-cm, and if the frequency of operation is less than 200 GHz, the Rayleigh approximation can be used to estimate the specific attenuation within a cloud or fog. Thus, the specific attenuation (dB/km) is given by:

$$\gamma_c = K_l M, \quad (20)$$

where:

γ_c: specific attenuation within the cloud (dB/km),

K_l: specific attenuation coefficient ((dB/km)/(g/m^3)), and

M: liquid water density in the cloud or fog (g/m^3).

To find the specific attenuation coefficient, K_l, a mathematical model based on the Rayleigh scattering was used. This model can be used to calculate the value of K_l for frequencies as high as 1,000 GHz. The equation for K_l is given by:

$$K_l = \frac{0.819f}{\varepsilon''(1+\eta^2)}, \tag{21}$$

where:

$$\eta = \frac{2+\varepsilon'}{\varepsilon''}, \tag{22}$$

$$\varepsilon''(f) = \frac{f(\varepsilon_0-\varepsilon_1)}{f_p[1+(f/f_p)^2]} + \frac{f(\varepsilon_1-\varepsilon_2)}{f_s[1+(f/f_s)^2]} \quad , \tag{23}$$

$$\varepsilon'(f) = \frac{\varepsilon_0-\varepsilon_1}{1+(f/f_p)^2} + \frac{\varepsilon_1-\varepsilon_2}{1+(f/f_s)^2} + \varepsilon_2 \ , \tag{24}$$

$$\varepsilon_o = 77.66 + 103.3\ (\theta - 1), \tag{25}$$

$$\varepsilon_1 = 0.0671\ \varepsilon_0, \tag{26}$$

$$\varepsilon_2 = 3.52, \tag{27}$$

$$\theta = 300 / T, \tag{28}$$

$$f_p = 20.20 - 146\ (\theta - 1) + 316\ (\theta - 1)^2 \text{ (GHz)}, \tag{29}$$

$$f_s = 39.8\ f_p \text{ (GHz)}, \tag{30}$$

T: temperature in Kelvin; and

f: frequency in GHz,

Temperature and the *liquid water density* are two factors required by the model.

3.1.3 Rain

A third factor affecting the propagating signal is the attenuation due to rain. To study the effect of that factor, the ITU-R "Specific Attenuation Model for Rain for use in Prediction Methods" was used [14]. According to the ITU-R reference, the specific attenuation (dB/km) due to the rain-rate can be calculated using the following:

$$\gamma_R = kR^\alpha \tag{31}$$

where:

$$k = \frac{[k_H + k_V + (k_H - k_V)cos^2\theta\ cos\ 2\ \tau]}{2}, \tag{32}$$

$$\alpha = \frac{[k_H\alpha_H + k_V\alpha_V + (k_H\alpha_H - k_V\alpha_V)cos^2\theta\ cos\ 2\ \tau]}{2k}, \tag{33}$$

γ_R: specific attenuation due to rain(dB/km),

R: rain rate (mm/h),

k: constant coefficient,

α: constant coefficient,

θ: path elevation angle,

τ: polarization tilt angle relative to the horizontal (τ = 45° for circular polarization),

k_H and α_H are constant coefficients for horizontal polarization, and

k_v and α_v are constant coefficients for vertical polarization.

Values for k_H, α_H, k_v and α_v for different frequencies were provided in the reference. An estimate of the rain-rate was required to calculate the attenuation.

3.2 Silva Mello Model

The path attenuation due to rain based on the Silva Mello model will now be explained. This model used the complete rainfall rate distribution, and the concepts of *effective path length* and *rainfall rate*. It has been shown that this method has significant improvement over the ITU-R method, because the ITU-R "underestimates the attenuation measured in terrestrial links, particularly for low latitude regions with severe rain regimes" [17]. Even though Albuquerque is not considered to be a region with a severe rain regime, a comparison between Silva Mello and ITU-R was made.

For the Silva Mello model, the equation used to calculate the attenuation due to rain is given by:

$$A = k[R_{eff}(R_p, d)]^{\alpha} \frac{d}{1+\frac{d}{d_0(Rp)}} \ (dB), \tag{34}$$

where:

$$R_{eff} = 1.763\ R^{0.753+0.197/d} \ \text{(effective rain rate)}, \tag{35}$$

$$d_0 = 119R^{-0.244} \ \text{(equivalent cell diameter)}, \tag{36}$$

d: actual path length (km), and (37)

R: rain rate (mm/h). (38)

The values of k and α were given by Olsen *et al*. [13]. The parameters k and α depend on the frequency of operation and the rain temperature. Values of k and α for four different distributions, which depend on the region of operation and the average drop size distribution, were presented reference [13]. These distributions were:

1) Laws and Parsons Distribution (LP): mainly used when the rain rate is below 35 mm/h in continental temperate rainfall with a mean drop size spectrum;
2) Marshall-Palmer Distribution (MP): mainly used for widespread rain in continental temperate climate (note that this distribution tends to overestimate the number of small drops);
3) Thunderstorm Distribution (JT): mainly used in convective rain (note that this distribution has not been extensively tested, but it has been used for some cases); and
4) Drizzle Distribution (JD): mainly used in regions having mostly small drops (note that this distribution is not generally used in communication systems purposes, because it accounts mostly for small droplets).

To increase the accuracy for the Laws and Parsons distribution, two regressions were performed. One regression takes into account low rain rates (LPL). The other takes into account high rain rates (LPH). Therefore, in total, five different distributions are available with which to estimate the values of k and α. These distributions include: LPL, LPH, MP, JT, and JD.

The values of k and α were given at specific frequencies for each distribution. Since the frequencies of interest (72 GHz and 82 GHz) were not included in the data provided, an interpolation was performed. In the tables given by Olsen et al. [13], the available data were given for specific rain temperatures, which included {-10 °C, 0 °C, and 20 °C}. Therefore, attenuation calculations were performed only for these rain temperatures. The equations given by the Silva Mello model were used to calculate the total attenuation.

3.3 Weather Data

For each model, weather data were required. For example, in order to calculate the attenuation due to atmospheric gases, the temperature, pressure, and water vapor density must be obtained. Most of the weather-related inputs were obtained from the Mesowest website [18]. However, the water vapor density was obtained through the use of data provided by the ITU-R website [19].

The Mesowest website is a database of weather stations that allows users to download the weather data from any of the weather stations provided. From this website, the time and dates for the temperature, pressure, and rain for each of the desired weather stations were obtained.

To calculate the attenuation for atmospheric gases, the water vapor density was required. This data was not provided by the Mesowest website. The ITU-R website provided a database of surface water vapor density values while an associated paper [20] described how to estimate the water vapor density at any location on earth and at any altitude. For the ITU model, the only required weather related input for rain attenuation was rain-rate, which was provided by the Mesowest website. For the Silva model, the required inputs were the rain-rate and the rain temperature. It was determined that the rain temperature can be estimated by the air temperature, which was provided by the Mesowest website. The ITU model for the attenuation due to clouds or fog required the cloud thickness or the liquid water density. At this point, a method for obtaining this information has not been determined. The data was simply estimated based on the temperature and humidity, with the maximum being 0.5 g/m^3 for *thick* clouds and the minimum being 0.05 g/m^3 for *medium* clouds.

To determine water vapor density, a water vapor density paper from ITU-R [20] was used. The paper detailed the steps to download the surface water vapor density values on a grid of latitude and longitude values for specific probabilities of exceedance. Next, the paper described how to use the data provided to bi-linearly extrapolate the values for any point on earth and at any altitude. Using the approach mentioned in the paper, a code was developed to calculate the water vapor density. The code finds the four closest latitude and longitude (by GPS) points to the desired points. Once it finds these global positioning system (GPS) points, it finds the four surface water vapor density values corresponding to the GPS points. It then finds the four vertical scaling factors corresponding to the GPS points. Then, it vertically scales the surface water vapor density values based on the altitudes of the four corresponding GPS points, the altitude of the desired GPS point, and the four vertical scaling factors. These new four values become the water vapor density values at the appropriate altitudes. Once the vertically scaled water vapor density values are obtained for the four corresponding GPS points, the vertically scaled water vapor density, or simply the water vapor density, was calculated by bi-linearly extrapolating from the four vertically scaled water vapor density values.

3.4 WTLE Experiment Description

The goal of WTLE is to build an experiment test range for 72 GHz and 82 GHz. The objective is to calculate signal attenuation and correlate to atmospheric factors and conditions. The transmitter would be placed at Sandia Peak, near Albuquerque, New Mexico. The receiver would be placed at COSMIAC (Configurable Space Microsystems Innovations and Applications Center) located in Albuquerque, New Mexico. This provides an inclined path (see Figure 1) where the receiver is at an altitude of 1.619-km (5,260 ft) (above sea level) and the transmitter is at an altitude of 3.255-km (10,670 ft). The projected distance between the transmitter and the receiver is approximately 22.5-km, and the actual path length is approximately 22.56-km. GPS coordinates for the sites are given in Table 1. The elevation angle is:

$$\varphi_1 = \arctan\left(\frac{3.255-1.619}{22.5}\right) \sim 0.726\, rad \sim 4.16^{\circ}. \tag{39}$$

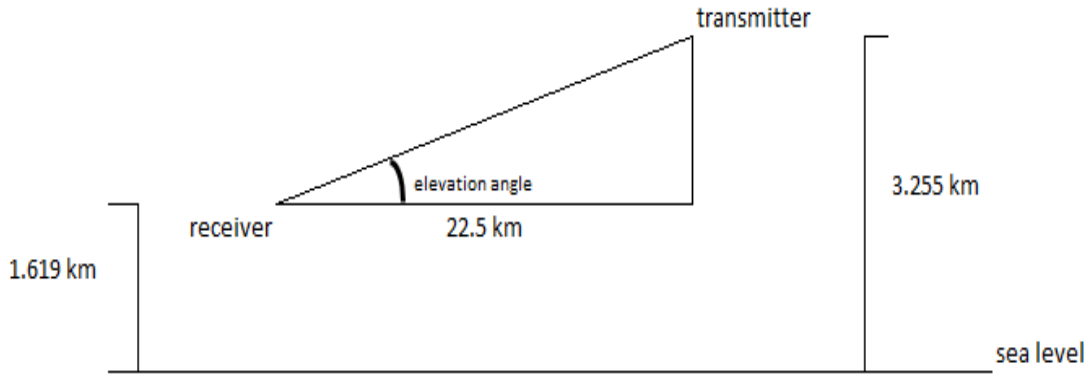

Figure 1. Geometry of WTLE Path

Table 1. Coordinates for WTLE Receiver and Transmitter Sites

	Receiver Site	Transmitter Site
Latitude	35°36.26’ N	35°12.7’ N
Longitude	106°37.1’ W	106°27’ W
Altitude (ft)	5,260	10,670

Weather data from three different weather stations located between the transmitter and the receiver along the path would be used for the experiment and for simulations. Figure 2 shows the relative locations of the primary weather stations along the path. Also shown are the locations of secondary weather station that can provide additional data for interpolation. The KABQ weather station is located near the COSMIAC building. The C8328 weather station is located near the intersection of the I-40 interstate and Louisiana Boulevard. The AR227 weather station is located near the intersection of Tramway Boulevard and Tramway Terrace Street. The distance between KABQ and C8328 is estimated to be 6.26-km. The distance between C8328 and AR227 is estimated to be 10.14-km. The distance between AR227 and Sandia Peak is estimated to be 6.2-km.

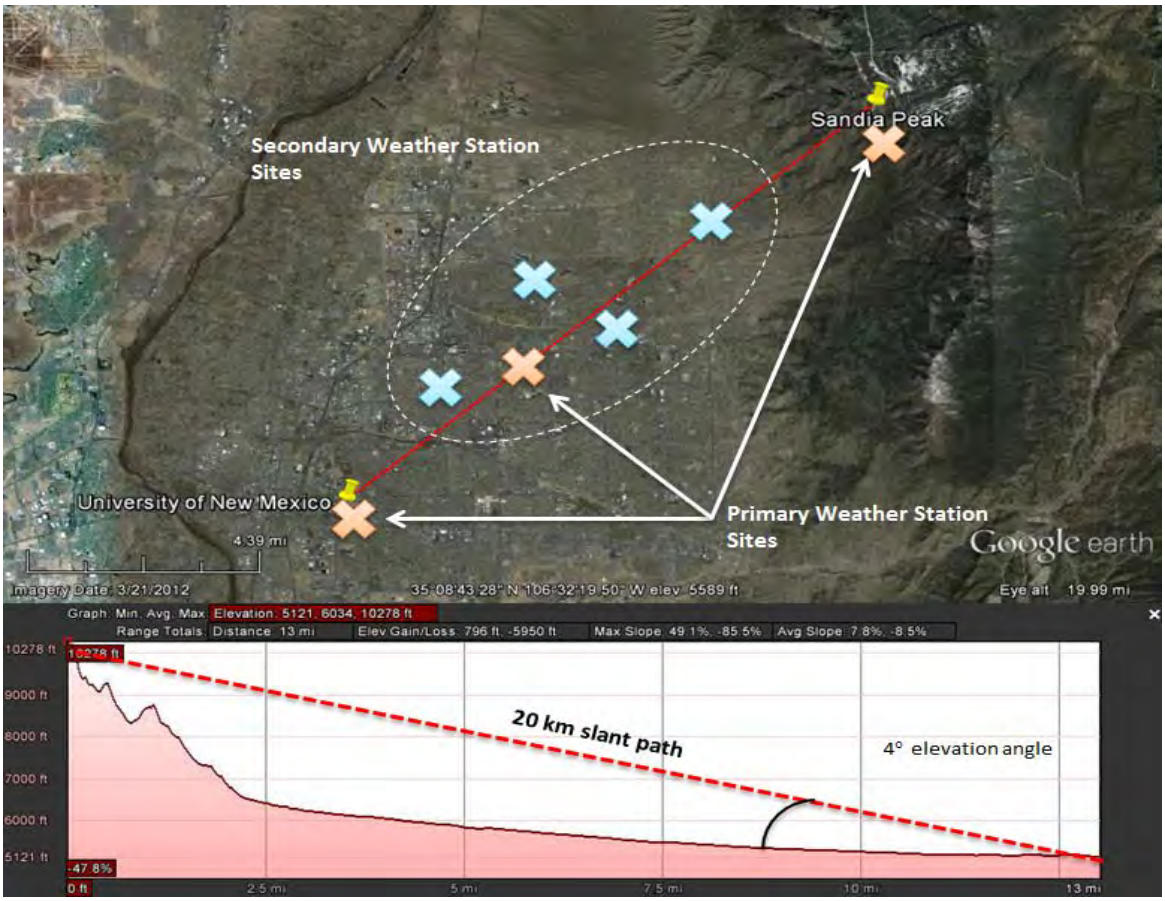

Figure 2. Location of Weather Stations

3.4.1 Transmitter Configuration

The WTLE transmitter assembly was acquired from Quinstar Technology, Inc. A block diagram is provided in Figure 3. The local oscillator (LO) (10 MHz) signal is split via a divider and routed to a phase-locked dielectric resonator oscillator (PLDRO) to generate the intermediate frequency (IF) (12 GHz) signal for both the W and V channels. The intermediate frequency signal is then up-converted to the carrier frequency and appropriately filtered. Signals are routed by waveguide (W/G) to a circular polarizer, and then coupled to lens antennas. A W/G power detector was included in the system electronics package to provide a measurement of power being delivered to the antennas.

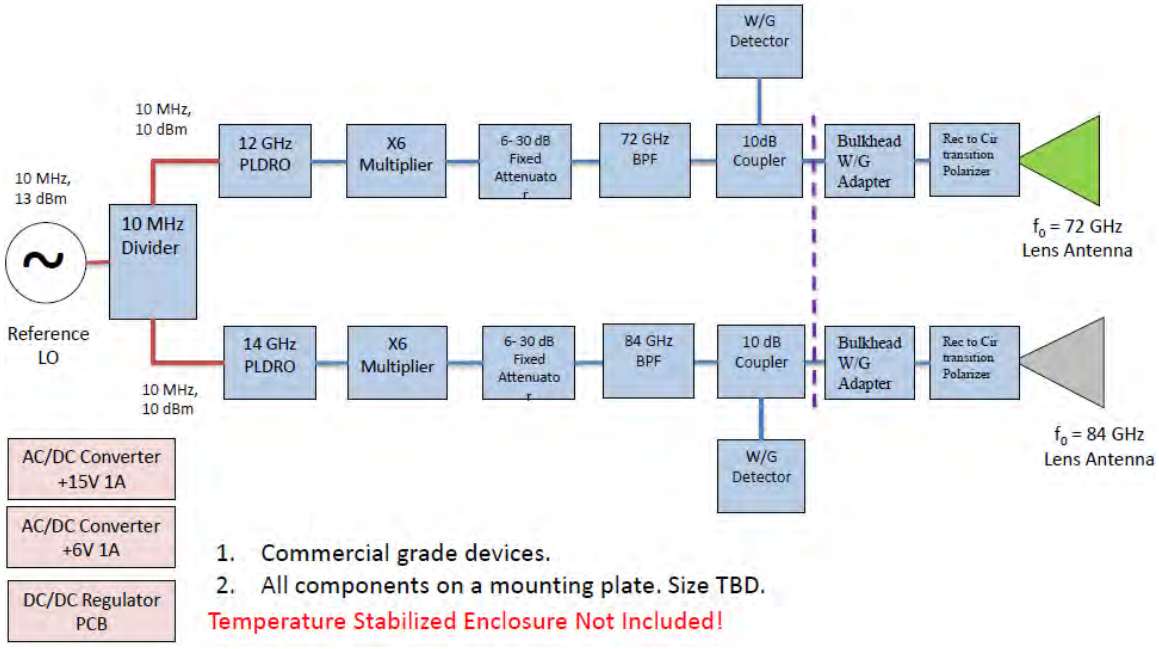

Figure 3. Transmitter Block Diagram

Quinstar characterized each component in the system and provided a detailed summary of the test results for the electronics package. A summary of performance is listed in Table 2. While some specifications were not met, the package should provide a stable and reliable beacon for WTLE. Figure 4 presents a picture of the completed transmitter electronics package with lens antennas. Figure 5 provides a schematic diagram of the transmitter package. The transmitter

would be located in a relatively harsh environment and requires a climate controlled external enclosure. Figure 6 shows the transmitter package inside an environmentally controlled enclosure.

Table 2. Transmitter Electronics Performance

System Parameters	Specification	V-band Test Result	W-band Test Result
Operating Frequencies	72 GHz (nom.) 84 GHz (nom.)	72.000,002,321	84.000,002,669
Antenna Half-Power Beamwidth (HPBW)	3° as a goal	3.6° (E/H)	3.2° (E)/3.0° (H)
EIRP	0 dBm/20 dBm (min.)(manually switchable). 3 dB difference between two frequency bands	41.1 (with 5 dB Attenuator)	40.4 (with 5 dB Attenuator)
EIRP Stability	+/- 0.05 dB (1 sec) +/- 0.1 dB (24 hrs)	-0.041 dBm/ °C	-0.073 dBm/ °C
Polarization	Single LHCP or RHCP	LHCP	LHCP
Axial Ratio	<1.5 dB	0.4	0.29
Cross-Pol Discrimination	>25 dB	32	35
LO Phase Noise	0.1 Hz -55 dBc 1.0 Hz -85 dBc 10 Hz -115 dBc 100 Hz -135 dBc	-74dBc/Hz -107 dBc/Hz -130 dBc/Hz -155 dBc/Hz	-74dBc/Hz -107 dBc/Hz -130 dBc/Hz -155 dBc/Hz
LO Frequency Stability	3.00E-12 (<100sec) 3.00E-9 (per day) 1.00E-7 (per year)	1.8E-11 5E-10	1.8E-11 5E-10
Air Temperature Stability	<0.1 °C rms	N/A	N/A

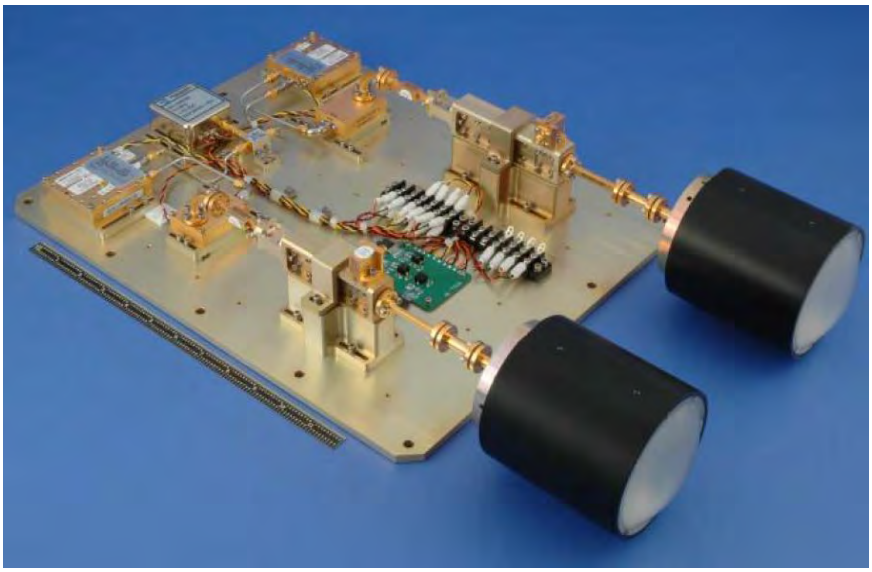

Figure 4. Picture of Transmitter Assembly

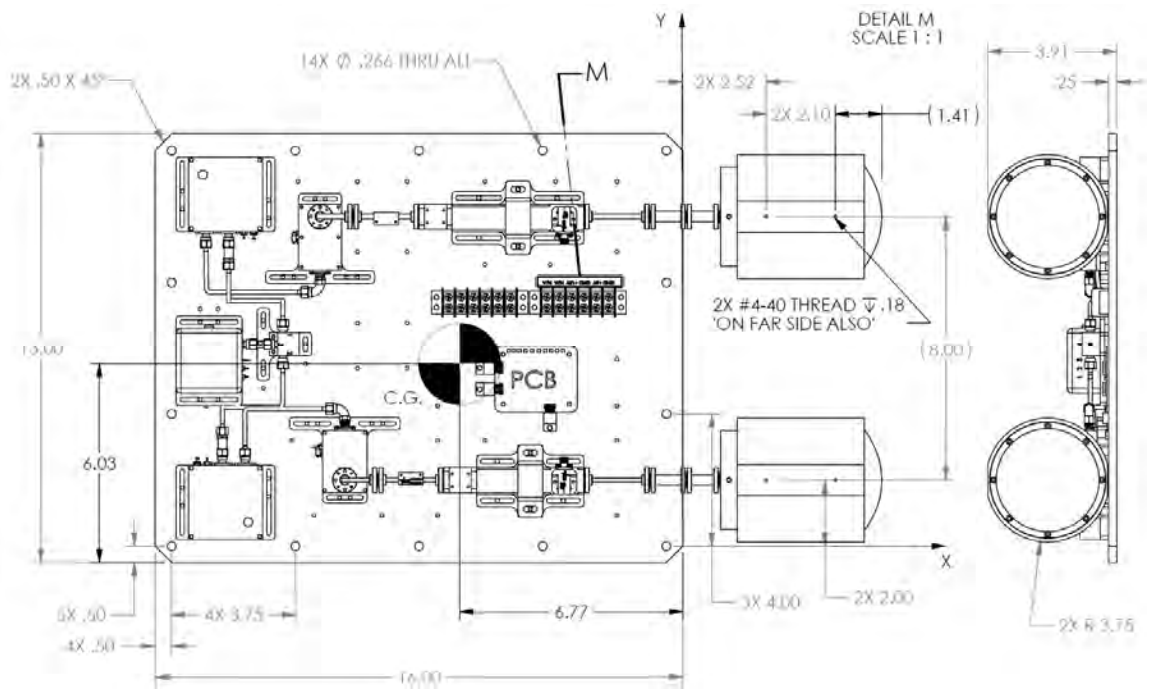

Figure 5. Schematic of Transmitter Assembly (units in inches)

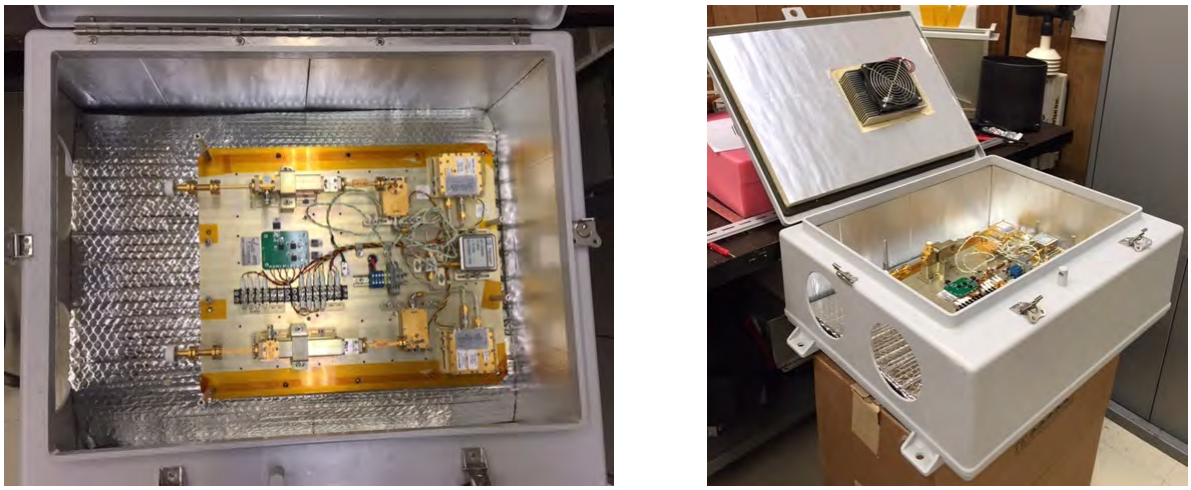

Figure 6. Transmitter Assembly in Environmentally Controlled Enclosure

3.4.2 Receiver Configuration

The receiver site for the WTLE experiment is more intricate and would include: (1) the receiver (Rx) antenna, (2) back-end radio frequency (RF) components, and (3) several atmospheric measurement devices. The atmospheric measurement devices would include: (1) a radiometer to provide an estimate of the attenuation, (2) a disdrometer to measure rain drop size distribution and velocity, and (3) a weather station. A component layout of the receiver system is shown in Figure 7.

A block diagram of the receiver electronics package is provided in Figure 8. The flow of the signal is, in general, exactly the opposite of the transmitter package. The antennas detect the beacon signal, which is bandpass filtered to the respective frequencies. The two paths are co-polarized left hand circular polarization (LHCP) on top and right hand circular polarization (RHCP) on bottom. The signals are then mixed with a phase-stable local RF source. A 72 GHz reference signal is generated in the receiver backend, and then routed through an externally controlled switch.

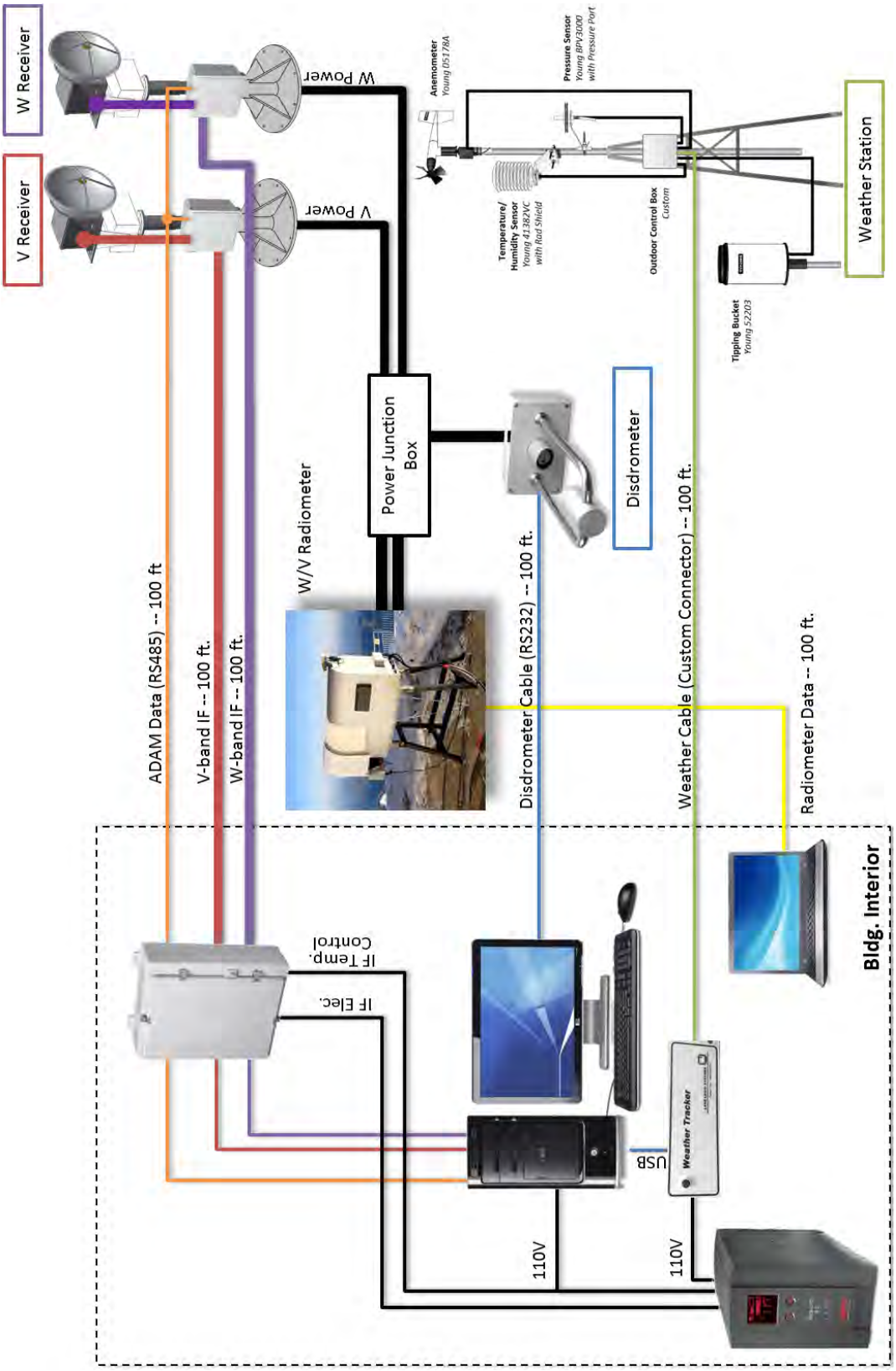

Figure 7. WTLE Receiver System

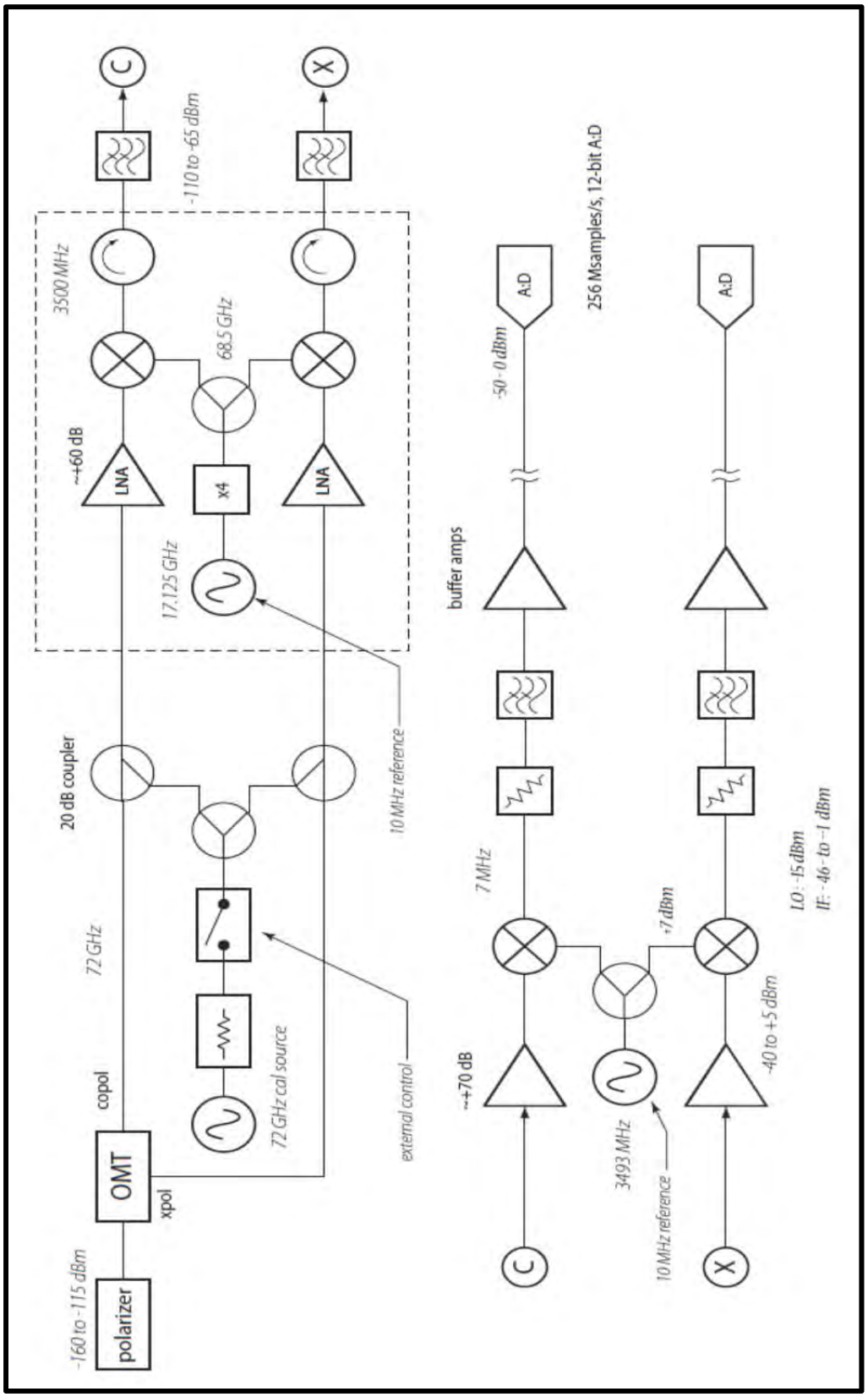

Figure 8. Receiver Block Diagram

3.5 Transmit Structure Displacement Measurement and Fortification

During initial Sandia Peak site visits, a concern was raised about the stability of the structure to be used for the WTLE transmit antenna assembly. The structure exhibited a very low and under-damped resonance frequency. Therefore, the structure was stiffened with braces that were secured to the roof of the building as shown in Figure 9. Weather instruments were attached to the reinforced structure as shown in Figure 10. Instruments included a barometric pressure sensor, rain gauge (i.e., tipping bucket), temperature and humidity probes, and wind monitor.

Figure 9. Fortification of WTLE Tx Antenna Mounting Structure; Before (Left) and After Brace Installation (Left)

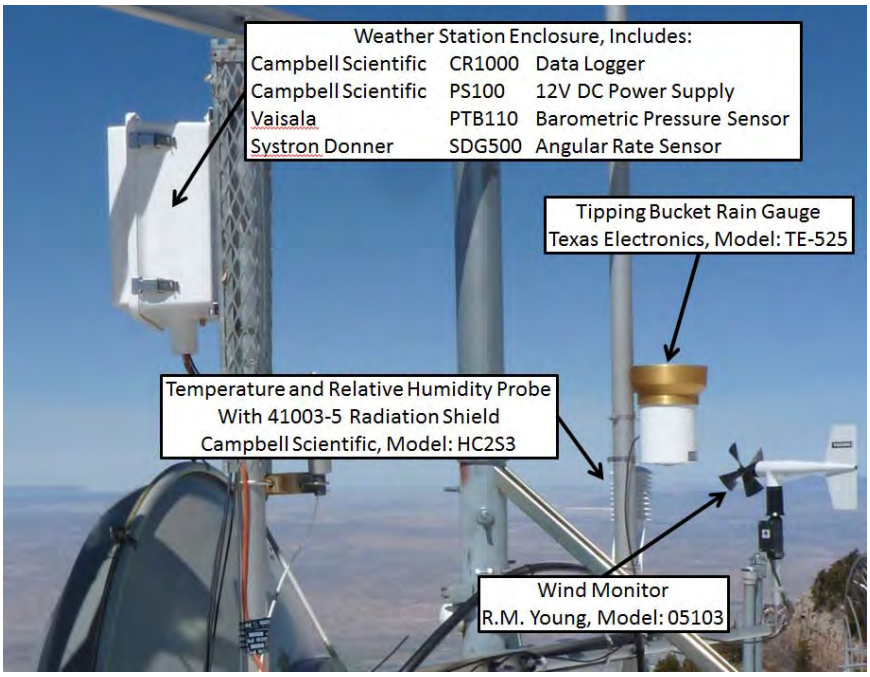

Figure 10. Weather Station Installed on Transmitter Structure

Angular displacement measurements of the transmit (Tx) and Rx antennas are required to enable us to separate signal degradations resulting from bore-sight pointing error and from atmospheric attenuation. Angular rate gyros were used to collect this data. These angular rate gyros and companion data recorder were also attached to the transmitter structure. Figure 11 shows the inside layout of that box.

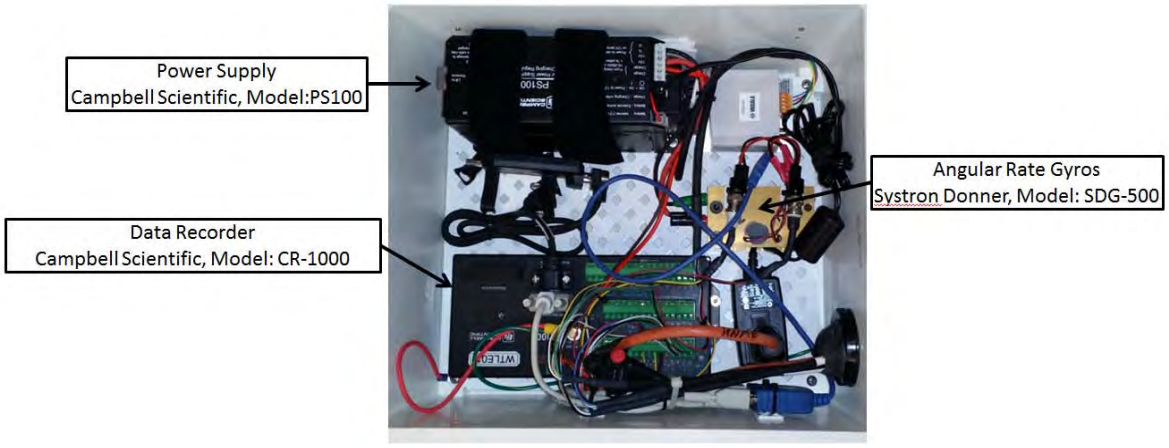

Figure 11. External Enclosure Internal Layout

Data was collected using weather station instruments during the time-period of 25-Mar-2015 to 10-Apr-2015. This test also allowed us to obtain an estimate of the magnitude of pointing errors to be expected at the transmit site. The data showed good correlation between the wind monitor and the gyro outputs, especially when the wind magnitude was normalized by the direction of the wind load on the structure. The data is presented in Figure 12. The magnitude of the recorded angular displacement was on the order of a tenth of a degree. Unfortunately, the data exhibited several anomalies. We are concerned that the current location may have very strong electromagnetic fields produced by neighboring transmitters, which may corrupt our instruments. If this is true, the WTLE transmit electronics may not perform adequately and a different site may have to be selected.

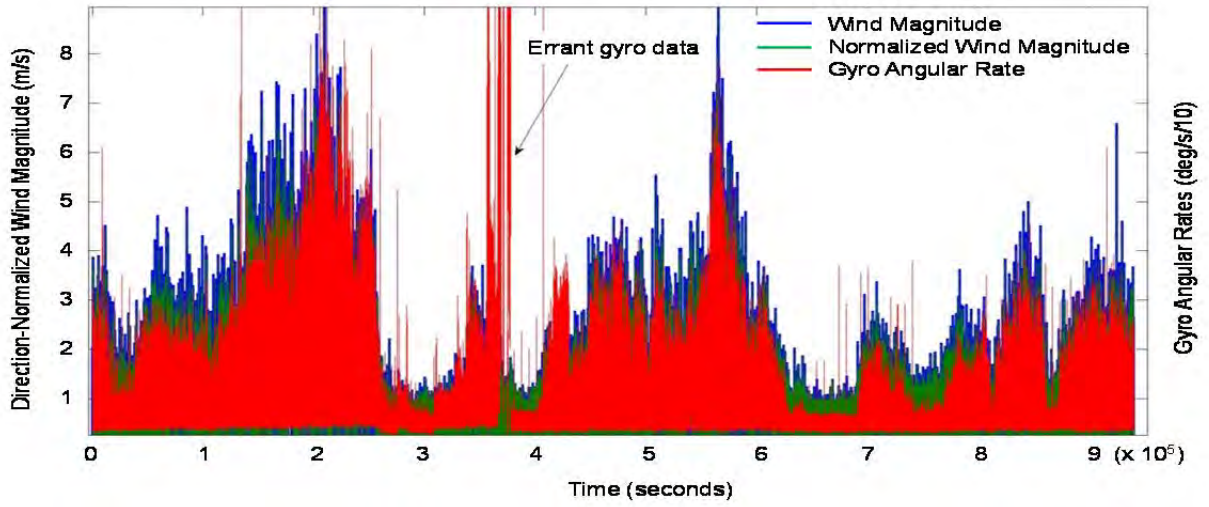

Figure 12. Time Traces of the Wind and Gyro Measurements

3.6 Anechoic Chamber Preparation

The WTLE lens antennas are to be measured and characterized by students in the Electrical and Computer Engineering Department at the University of New Mexico (UNM/ECE). Preparation of the UNM/ECE anechoic chamber for high frequency measurements included the design of a transmit antenna mount, shown in Figure 13. The mount provides a means to ensure that the output aperture of the device under test is centered directly over the rotating positioner. It

allows for adjustment in all linear directions. The antenna mount was fabricated out of plastic. Additionally, the hardware that secures the mount was also fabricated from plastic to reduce interference with the device under measurement.

Figure 13. Solid Model of Anechoic Chamber Tx Antenna Mount Assembly

Another important consideration for antenna measurements is the orthogonality of the Tx and Rx antennas. The antenna mount allows for fine-tune adjustment of the *y*-axis rotation, as shown in Figure 14. Rotation in the *z*-axis is controlled by a Lindgren Model 5000 rotation positioner. When the antenna is at the desired height in the *z*-axis, the nut on the bottom post of the yellow disc can be tightened. The nut on the post provides a pivot-point for the yellow disc to be rotated along the curved slot until the antenna is perpendicular, at which point the upper post is then secured.

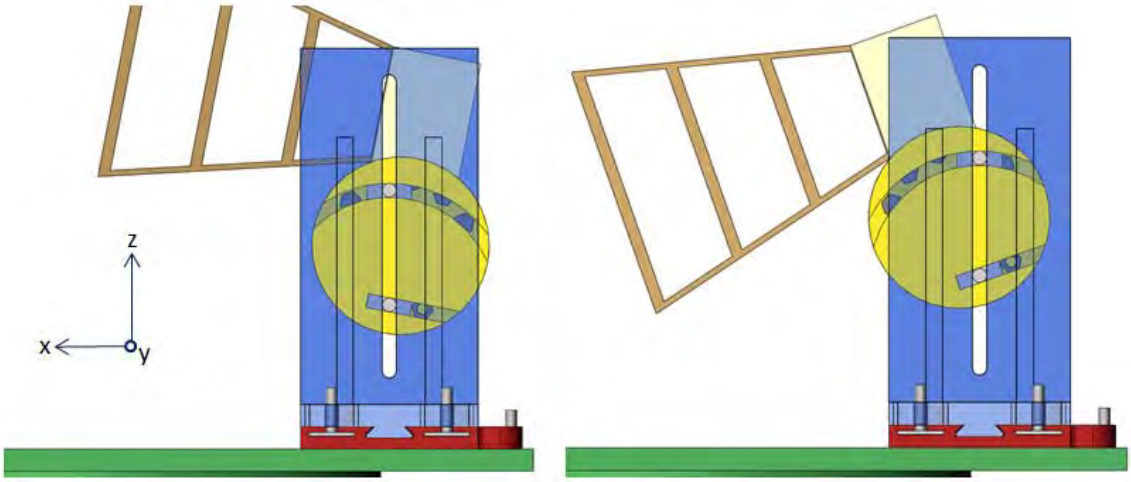

Figure 14. Tx Antenna Mount, Adjustment to Ensure Tx and Rx Antenna Orthogonality

The antenna mount has a feature to allow multiple slices of the antenna to be measured, which allows for 3-D antenna pattern measurement. Both the yellow discs and a central mount located between the yellow discs have holes spaced at 30° increments. Nuts permanently located on the back side of the yellow discs can be used to secure a bolt from the central mount to the yellow disc. Figure 15, shows how the holes in the central disc (shown in transparent gray) line up with the holes on the yellow discs.

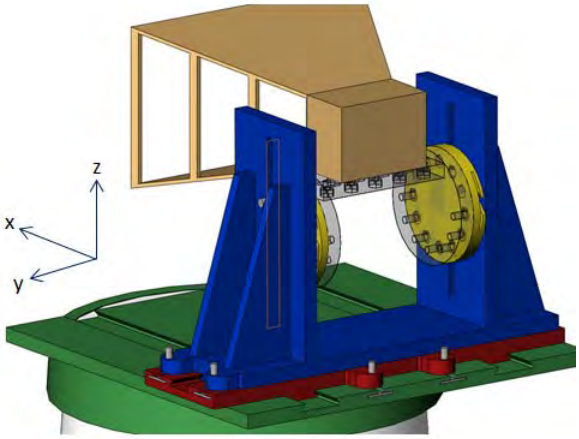

Figure 15. Tx Antenna Mount, Adjustment for 3-D Antenna Measurements

A final consideration for antenna measurements is the development of an alignment system to ensure the Tx and Rx antennas are perpendicular and vertically aligned. The system is shown in Figure 16. We use a small laser to accurately position the device under test. Once aligned, the laser alignment system can be removed from the antenna mount.

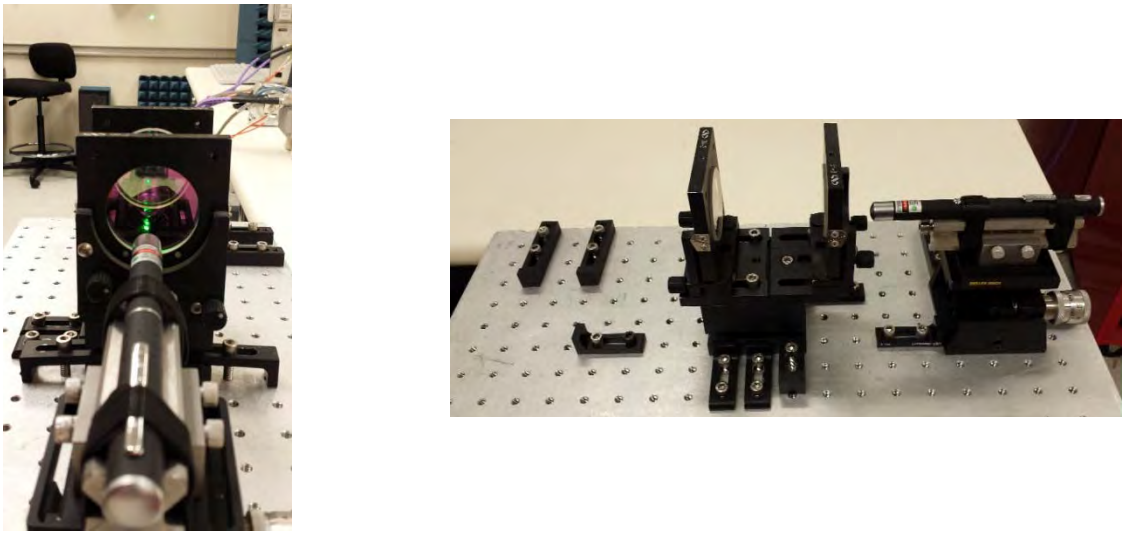

Figure 16. Laser Alignment Setup

4 RESULTS AND DISCUSSION

This section provides preliminary simulation results for the ITU-R and Silva Mello model. Analysis of the models and simulations continues. However, some qualitative observations can be made.

4.1 ITU-R Models

The simulation results for the ITU-R models are shown for 72 GHz and 82 GHz in Figure 17 and Figure 18, respectively. The water vapor density was assumed to be 7.442 g/m^3 for a 1% probability exceedance during the month of April in the city of Albuquerque, NM. In other words, 99% of the month of April, the water vapor density would be 7.442 g/m^3 or less. The predicted temperature, pressure, precipitation, cloud thickness, and attenuation were computed for the three weather station location previously described. The results indicate that for the rain

and cloud weather factors, the attenuation at 82 GHz is higher than the attenuation at 72 GHz, as would be expected, since attenuation due to weather increases with frequency. As for the atmospheric gas factor, the attenuation at 82 GHz is lower than the attenuation at 72 GHz, as would be expected, since 82 GHz is farther from the oxygen absorption complex. The difference between the two frequencies decreases with a decrease in temperature. Thus, the models appear to be working as expected.

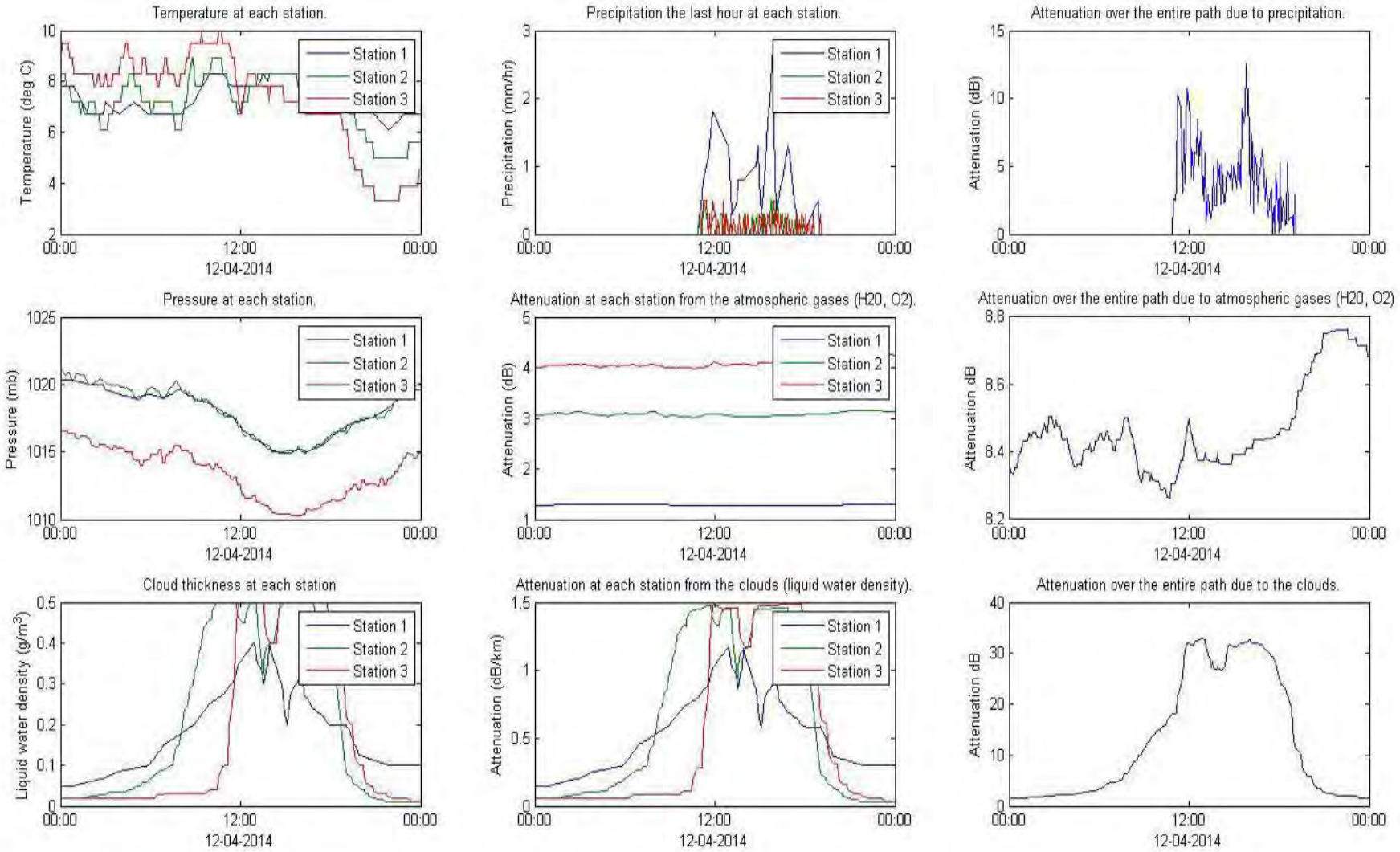

Figure 17. ITU-R Models Results for *f* = 72 GHz

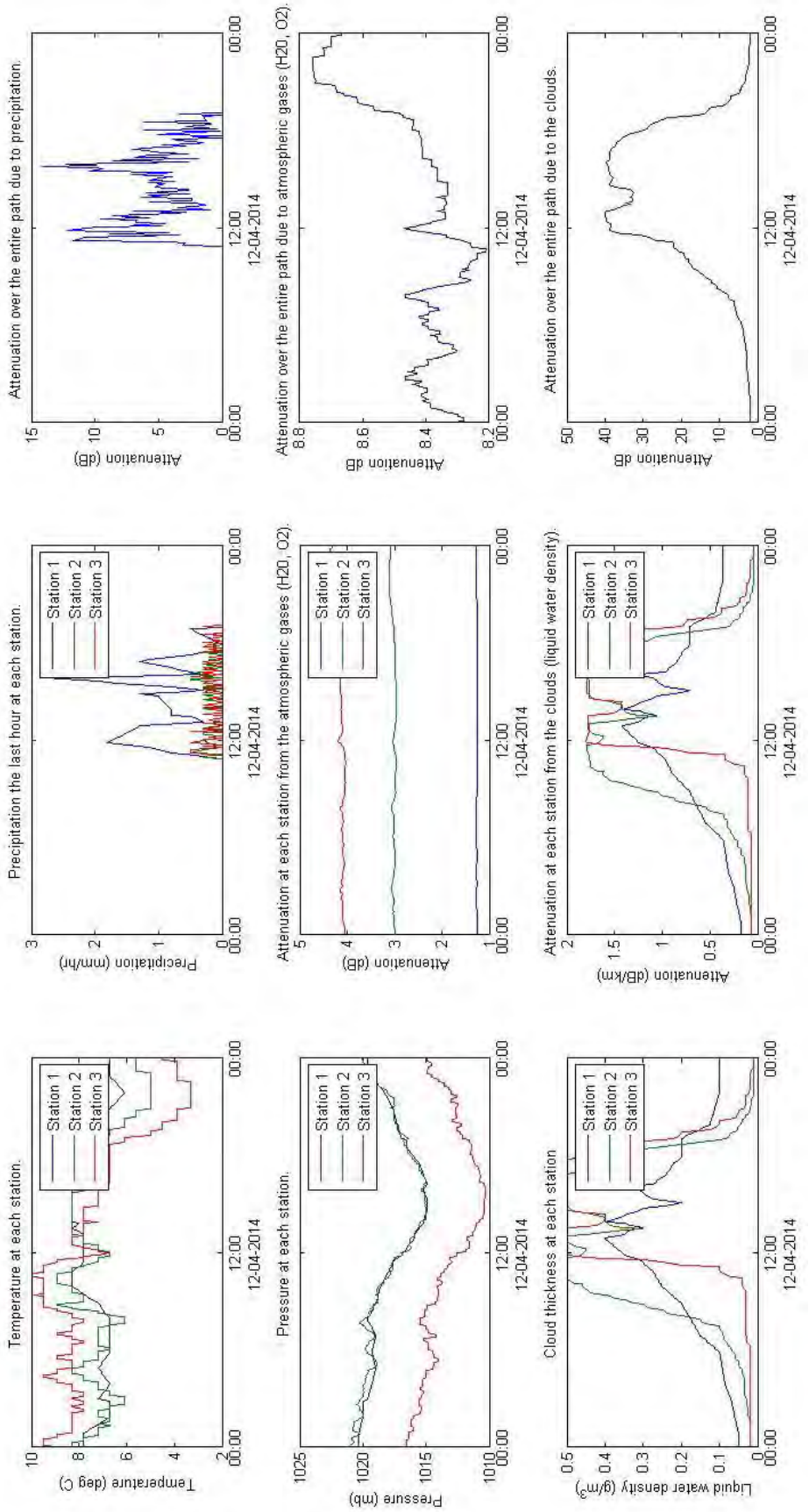

Figure 18. ITU-R Models Results for f = 82 GHz

4.2 Silva Mello Model

Using the framework discussed earlier, representative variations of temperature and rain-rate as a function of time were simulated and are presented in Figure 19. Temperature and precipitation were computed for the three ground station locations planned for the WTLE experiment. The simulations depict a rain event occurring in the afternoon. Station 1 is clearly expected to experience the greatest amount of precipitation.

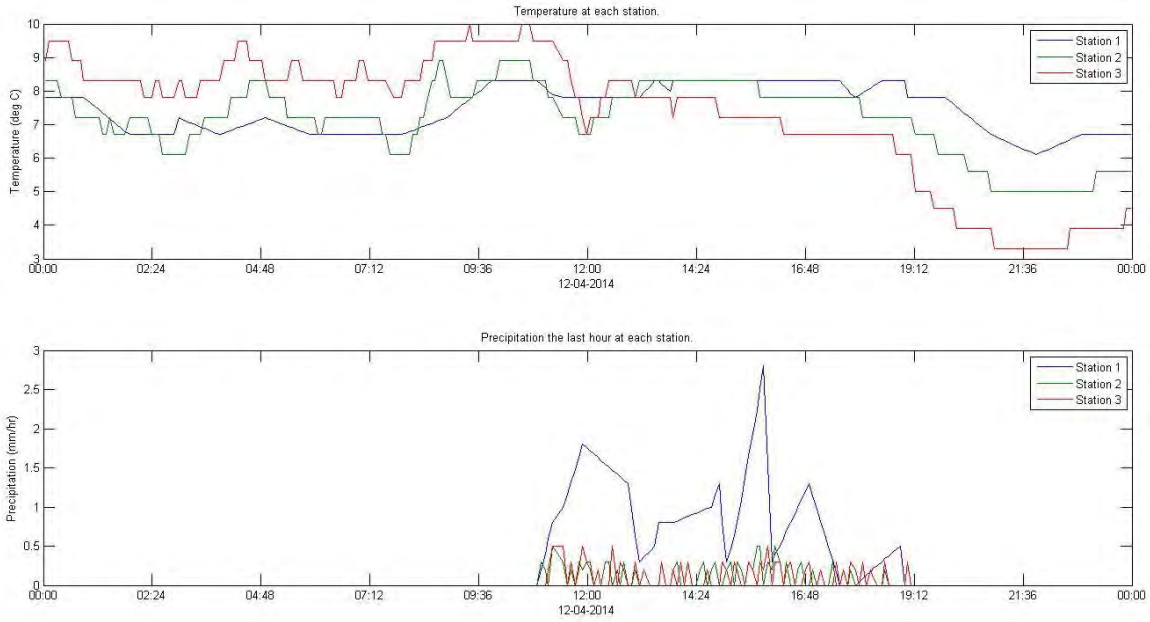

Figure 19. Temperature and Rain-Rate as a Function of Time

From the assumed (representative) temperature and precipitation profiles, the *total attenuation* for the WTLE link was simulated. Each subsequent simulation compares the estimated total attenuation for all 5 distributions discussed previously (i.e., Laws and Parsons (LPL & LPH), Marshall-Palmer (MP), Thunderstorm (JT), and Drizzle (JD)). For each frequency, simulations were conducted assuming three different rain temperatures {0 °C, -10 °C, and 20 °C}. Figure 20 shows the results for 72 GHz at a rain temperature of 0 °C. Figure 21 corresponds to 72 GHz and rain temperature of -10 °C. Figure 22 corresponds 72 GHz and rain

temperature of 20 °C. Figure 23, Figure 24, and Figure 25 present the simulation results at 82 GHz for {0 °C, -10 °C, and 20 °C}, respectively. As expected, there is significant fluctuation of the total path attenuation during the rain event. In all cases, the Marshall-Palmer distribution resulted in the greatest attenuation prediction. The simulations indicate that total attenuation can exceed 20 dB for the given rain-rate at 72 GHz. The simulations also suggest that total attenuation can approach 30 dB at the given rain-rate at 82 GHz. Further quantitative analysis of the simulation results is underway. Qualitatively, it appears that the Silva Mello model did predict higher attenuation than the ITU-R model for both frequencies.

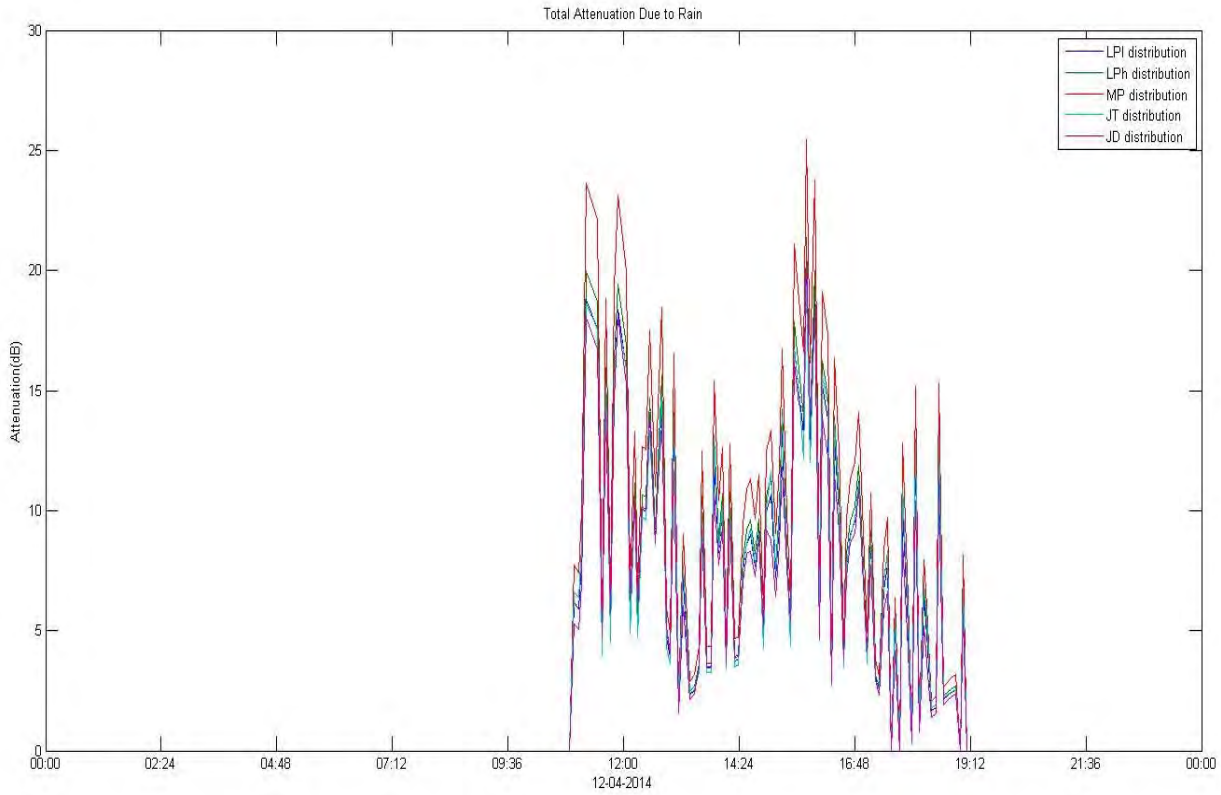

Figure 20. Silva-Model Results at *f* = 72 GHz and Rain Temperature = 0°C

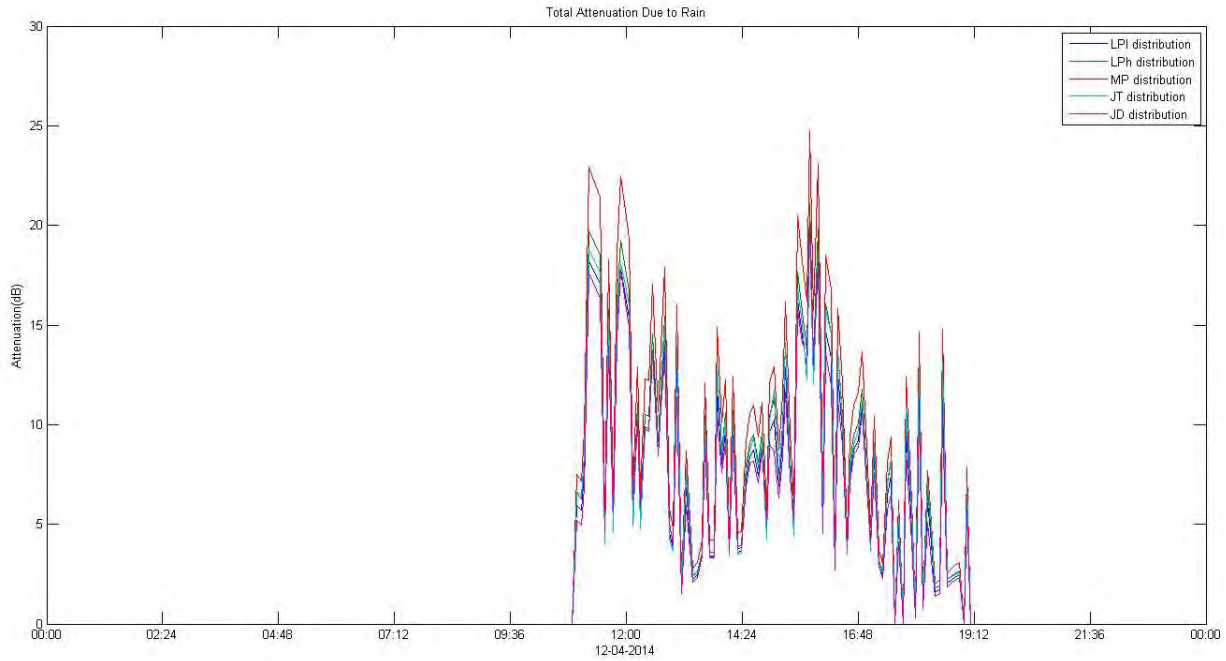

Figure 21. Silva-Model Results at *f* = 72 GHz and Rain Temperature = -10 °C

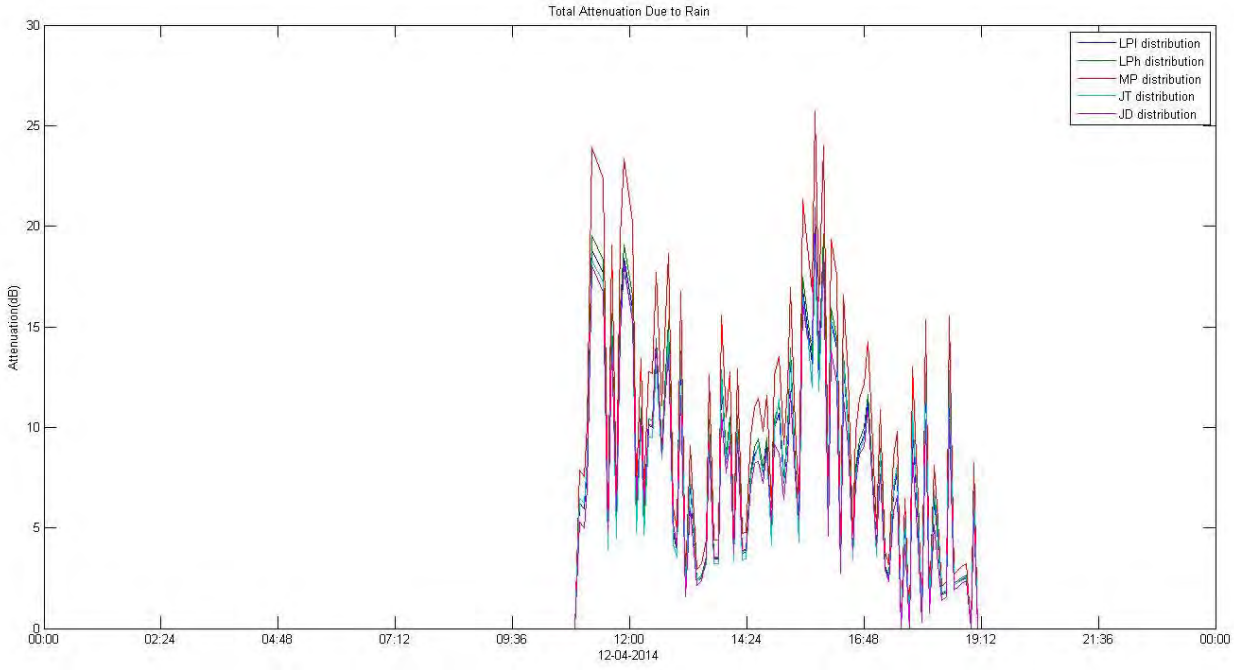

Figure 22. Silva-Model Results at *f* = 72 GHz and Rain Temperature = 20 °C

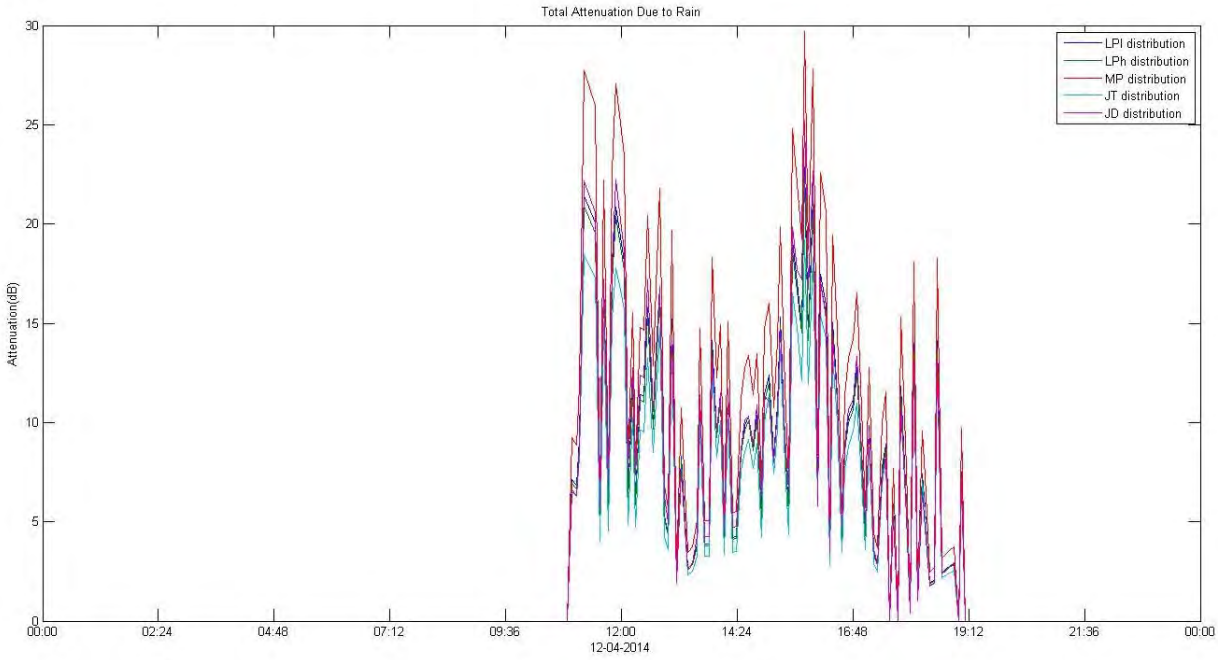

Figure 23. Silva-Model Results at *f* = 82 GHz and Rain Temperature = 0 °C

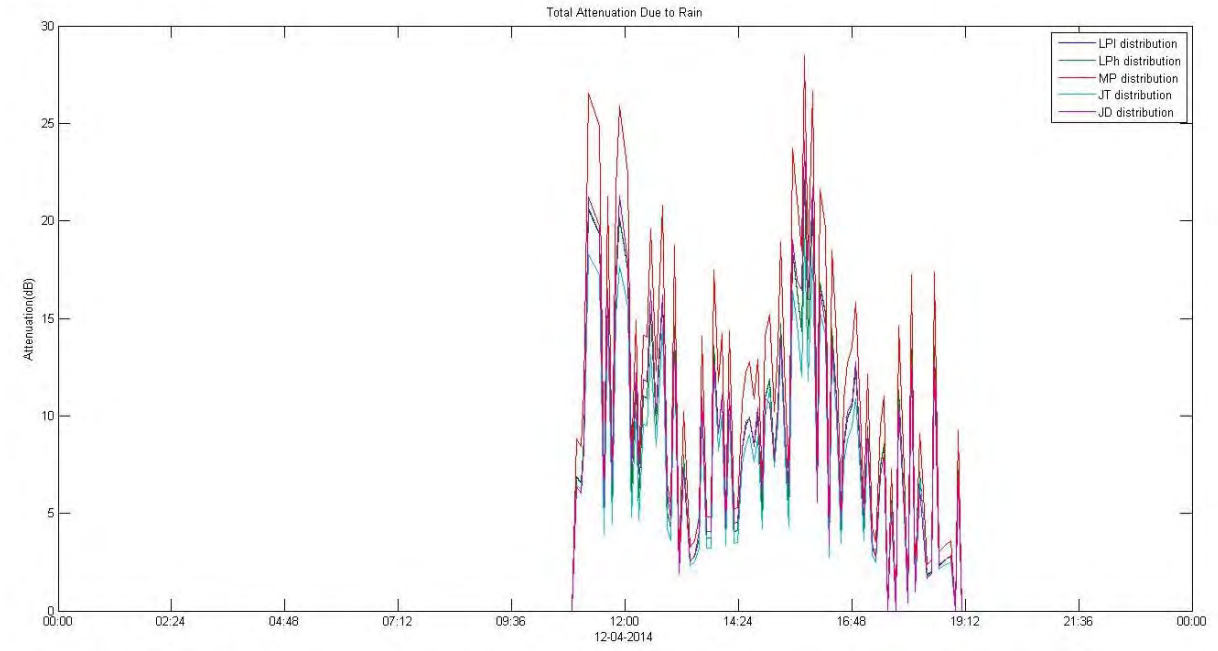

Figure 24. Silva-Model Results at *f* = 82 GHz and Rain Temperature = -10 °C

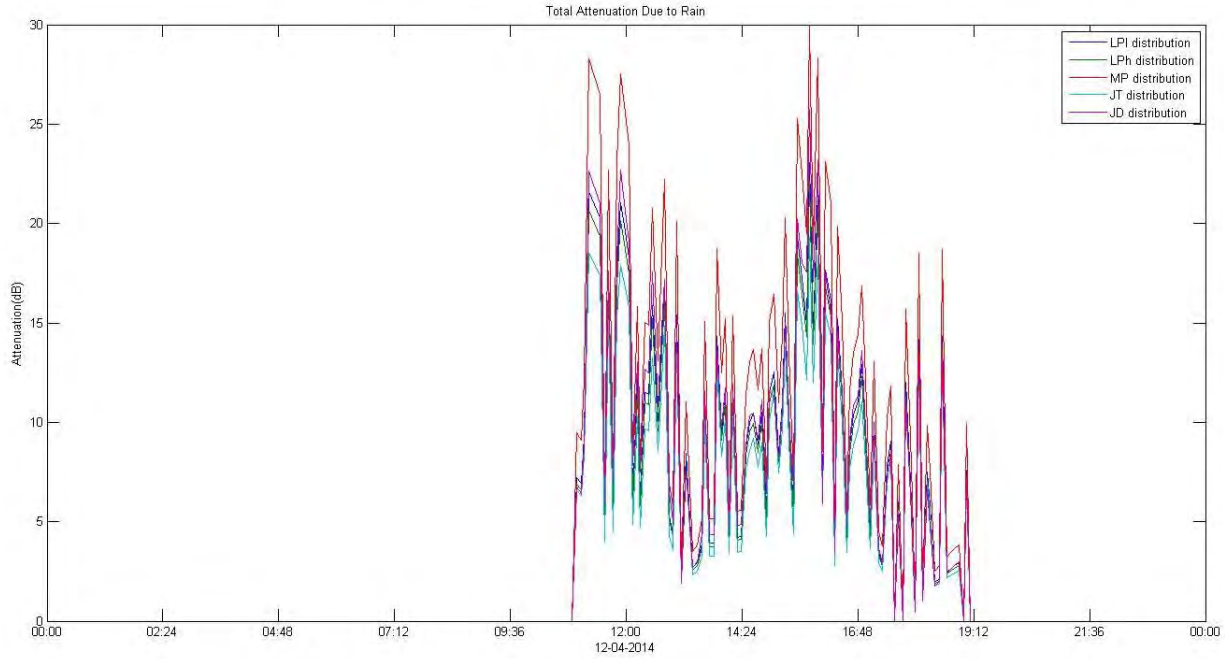

Figure 25. Silva-Model Results at *f* = 82 GHz and Rain Temperature = 20 °C

5 CONCLUSIONS

This work presented the well-known ITU-R model for atmospheric propagation attenuation and a model developed by Silva Mello. Each model included absorption from gases, water vapor, clouds, and precipitation. Simulation results were consistent with qualitative expectations. The models were applied to the proposed W/V-band Terrestrial Link Experiment (WTLE) concept. Simulation results suggest that low values of rain-rate (i.e., 2-3 mm/hr) could produce more than 20 dB of total link attenuation for the WTLE propagation path. As expected, attenuation increases with frequency.

The WTLE concept to experimentally validate and verify our models was described. WTLE consists of a tonal transmitter and companion receiver separated by 22.5 km and including a 4.5° inclination. WTLE would collect meteorology data along the propagation path and attempt to correlate signal attenuation to measured weather parameters.

Test facilities to measure antenna performance have been established and are functional. Likewise, transmitter and receiver systems have been developed and are currently being installed

and tested. Weather instruments are also being installed and tested. To mitigate experiment uncertainty, motion (angular rate) sensors have been installed on the mounting structures, which would enable de-correlation of pointing error from the test data.

6 RECOMMENDATIONS

We recommend that additional modeling approaches be investigated, which may provide valuable insight on the uncertainty at our target frequency range. New modeling tools are required to extrapolate available measurements to the actual propagation path parameters. We anticipate that actual data collection on the WTLE system will begin in August 2015. We recommend that data be collected under many operation conditions. We recommend that the data be analyzed to determine statistical trends and experimental uncertainty.

REFERENCES

1. G. E. Weible and H. O. Dressel, "Propagation Studies in Millimeter Wave Link Systems," *Proc. IEEE*, 55, No. 4, pp. 497-512 (1967).

2. K. L. Ho, N. D. Mavrokoukoulakis, and R. S. Cole, "Propagation Studies on a Line-of-Sight Microwave Link at 36 GHz and 110 GHz," *Microwaves Optics and Acoustics*, 3, No. 3. pp. 93-97 (1979).

3. J. H. Buys and L.H. Janssen, "Comparison of Simultaneous Atmospheric Attenuation Measurement at Visible Light, Mid-infrared (3-5 μm), and Millimeter Waves (94 GHz)," *IEEE Proc*. 128, Pt. H., No. 3, pp. 131-136 (1981).

4. W. P. Keizer, J. Snieder, and C. D. deHaan, "Rain Attenuation Measurement at 94GHz; Comparison of Theory and Experiment," *Advisory Group for Aerospace Research and Development* (*AGARD) Conf. Proc.*, No. 254, pp. 44-1/44-9 (1978).

5. M. Islam, Z. Elabdin, O. Elshaikh, O. Khalifa, A. Zahirul, S. Khan, and A. Naji. "Prediction of Signal Attenuation Due to Dust Storms Using Mie Scattering," *International Islamic University Malaysia (IIUM) Engineering Journal*, Vol. 11, No. 1, 2010.

6. J. Goldhirsh, "Attenuation and Backscatter from a Derived Two-Dimensional Dust Storm Model," *IEEE Trans. Antennas Propagation*, Vol. 49, No. 12, pp. 1703-1711, 2001.

7. Study Group 3 – Radiowave Propagation, "Recommendation ITU-R P.618-10: Propagation Data and Prediction Methods Required for the Design of Earth-Space Telecommunication Systems," 2009, PDF file.

8. R. Acosta, and J. Banks, "Advanced Communications Technology Satellite (ACTS)," National Aeronautics and Space Administration, Nov. 2009, World-Wide-Web. Oct. 2013.

9. Allnutt, J.E., *Satellite-to-Ground Radiowave Propagation*, 2nd Edition, London, United Kingdom, Published by the Institution of Engineering and Technology, 2011.

10. Study Group 3 – Radiowave Propagation, "Recommendation ITU-R P.676-9: Attenuation by Atmospheric Gases," 2012.

11. Study Group 3 – Radiowave Propagation, "Recommendation ITU-R P.836-4: Water vapor: Surface Density and Total Columnar Content," 2009.

12. Elert, G., "Diameter of a Raindrop," Hypertext. 2001. Web. http://hypertextbook.com.

13. R. Olsen, D. Rogers, and D. Hodge, "The αR^b Relation in the Calculation of Rain Attenuation," *IEEE Transaction on Antenna and Propagation*, Vol. AP-26, No. 2, pp. 318-329, March 1978.

14. Recommendation ITU-R P.838-3 (2005, March), "Specific Attenuation Model for Rain for use in Prediction Methods," http://www.itu.int/rec/R-REC-P.838-3-200503-I/en.

15. Recommendation ITU-R P.676-10 (2013, September), "Attenuation by Atmospheric Gases," http://www.itu.int/rec/R-REC-P.676-10-201309-I/en.

16. Recommendation ITU-R P.840-6 (2013, September), "Attenuation Due to Clouds and Fog," http://www.itu.int/rec/R-REC-P.840-6-201309-I/en.

17. L.A.R. da Silva Mello, M.S. Pontes, R.M. de Souza, and N.A. Perez Garcia (2007), "Prediction of Rain Attenuation in Terrestrial Links Using Rainfall Rate Distribution," http://ieeexplore.ieee.org/stamp/stamp.jsp?arnumber=4405611.

18. Mesowest, <http://mesowest.utah.edu/cgi-bin/droman/mesomap.cgi?state=NM&rawsflag=3>, October 2014.

19. ITU-R, <http://www.itu.int/rec/R-REC-P/en>, October 2014.

20. Recommendation ITU-R P.836-5 (2013, September), "Water Vapour: Surface Density and Total Columnar Content," http://www.itu.int/rec/R-REC-P.836-5-201309-I/en.

LIST OF SYMBOLS, ABBREVIATIONS, AND ACRONYMS

3-D	Three Dimensions
AC	Alternating Current
BPF	Band Pass Filter
°C	Degree Celsius
cm	Centimeter
COSMIAC	Configurable Space Microsystems Innovations and Applications Center
dB	Decibel
dBc	Decibels Relative to the Carrier
dBm	Decibel (relative to milli-Watt)
DC	Direct Current
deg	Degree
ECE	Electrical and Computer Engineering Department
E/H	Electric to Magnetic Field Amplitude
EIRP	Effective Isotropic Radiated Power
f	Frequency
ft	feet
g/m^3	Density, grams per cubic meter
Gbps	Gigabit per second
GHz	Giga-Hertz
GPS	Global Positioning System
HPBW	Half Power Beam Width
hr	hour
Hz	Hertz
IF	Intermediate Frequency
ITU-R	International Telecommunications Union (Radio)
JD	Drizzle Distribution
JT	Thunderstorm Distribution
km	kilometer
LHCP	Left Hand Circular Polarization
LNA	Low Noise Amplifier
LO	Local Oscillator

LP	Laws and Parsons
LPH	Laws and Parsons, High
LPL	Laws and Parsons, Low
MHz	Mega Hertz
mm	millimeter
MP	Marshal Palmer Distribution
m/s	Meters per second
PCB	Printed Circuit Board
PLDRO	Phase-Locked Dielectric Resonator Oscillator
Rec	Receiver
RF	Radio Frequency
RHCP	Right Hand Circular Polarization
Rx	Receiver
TBD	To Be Determined
Tx	Transmitter
UNM	University of New Mexico
USB	Universal Serial Bus
W/G	Wave Guide
WTLE	W/V-band Terrestrial Link Experiment

DISTRIBUTION LIST

DTIC/OCP
8725 John J. Kingman Rd, Suite 0944
Ft Belvoir, VA 22060-6218 1 cy

AFRL/RVIL
Kirtland AFB, NM 87117-5776 2 cys

Official Record Copy
AFRL/RVSV/Steven A. Lane 1 cy

(This page intentionally left blank)